A. Raman characterization of graphene bubbles

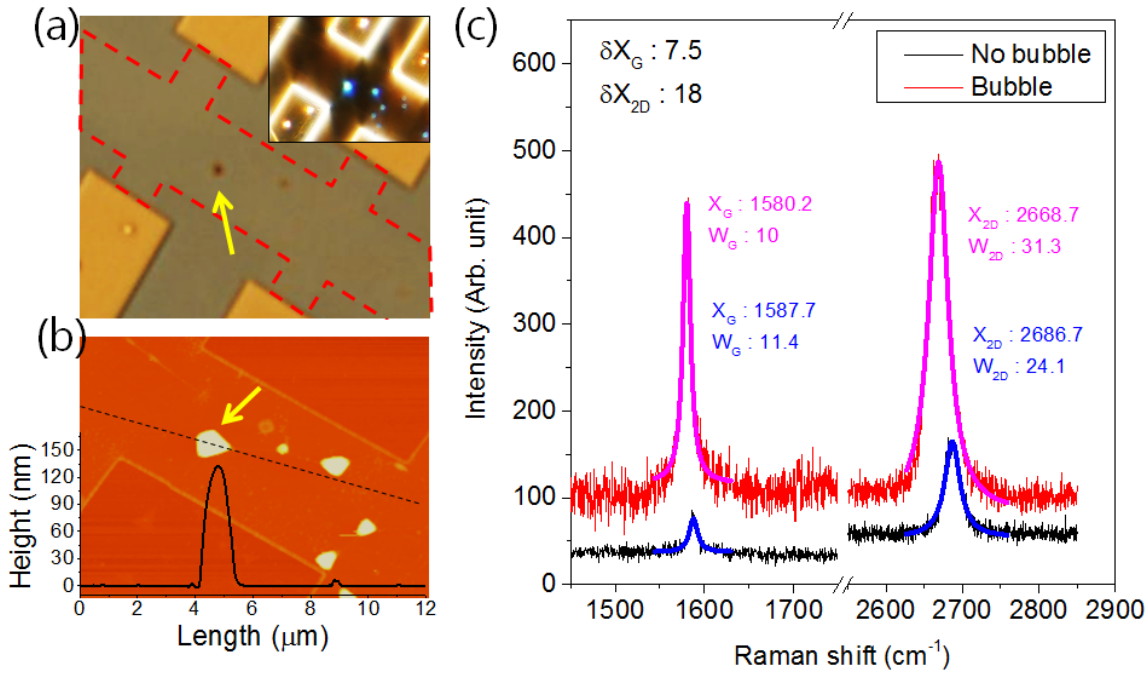

We carried out Raman spectrum measurement to clarify if we can practically differentiate the effects from chemical doping and the strains around bubbles in Raman signals. It is expected that G and 2D peaks are shifted to higher frequencies (blue shift) for p-type dopants, while those peaks are shifted to lower frequencies (red shift) under strains [1, 2]. Figure S1(c) shows the Raman spectrums measured at a bubble and bubble-free graphene. The optical view graphs and the AFM profile of the devices and graphene bubbles are shown in Fig. S1 (a) and (b), respectively. As shown in Fig. S1(c), both G and 2D peaks at the bubble are shifted to lower frequencies by 7 cm-1 and 18 cm-1, respectively, with respect to the positions from the bubble-free area. Figures S2 show the spatial profile of the intensity and the peak position of the G and 2D peaks from the device shown in Fig. S1, revealing that Raman signals are enhanced at the bubble region compared to bubble-free flat graphene area. The red-shifted G and 2D peaks around the bubble, located in the middle of the channel, are clearly identified, proving that strains are indeed built around graphene bubbles.

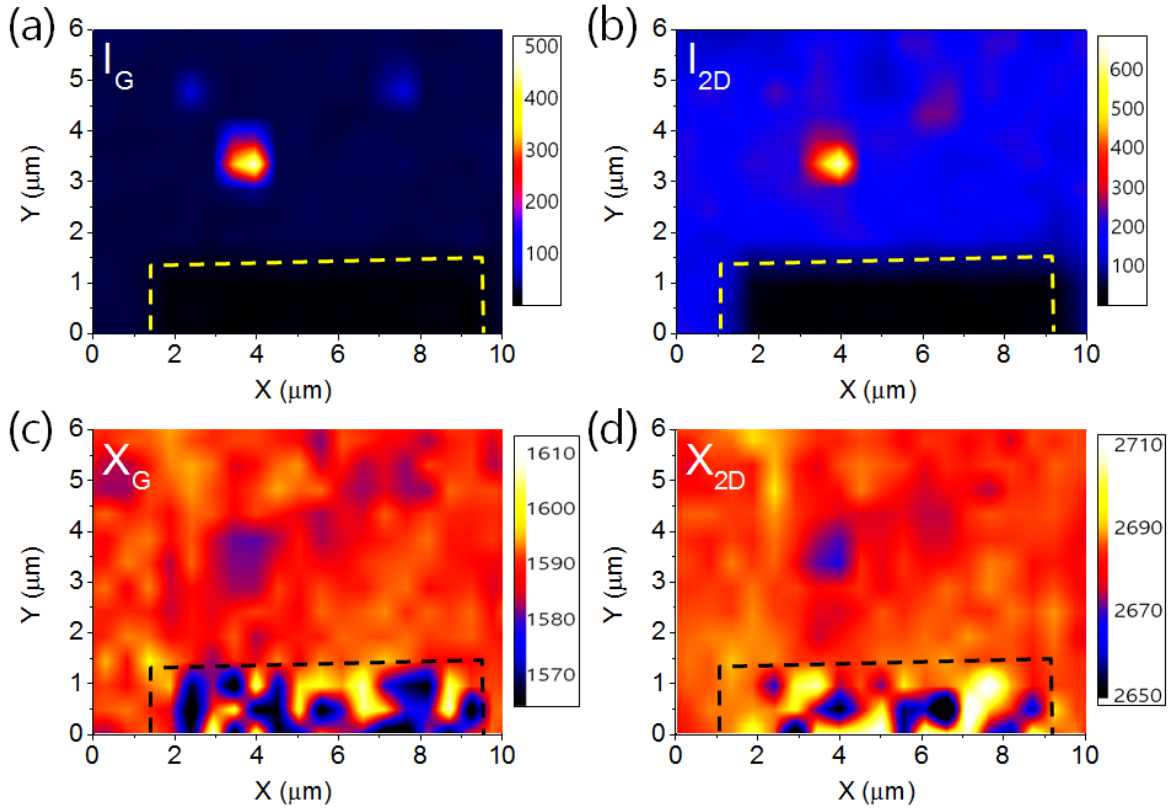

However, we need to note that Raman signals relating to p-type dopants from graphene bubbles, expected as the blue-shifted G and 2D peaks are easily overshadowed by the strain effects because Raman measurements are more sensitive to lattice distortions; strains than chemical impurities [3, 4]. Both G and 2D peaks are expected to shift to higher frequencies by just 1 cm-1 to 2 cm-1 from the p-type dopants of 5.3×1011 cm-2, equivalent for the device with a 5.9% bubble coverage, inspected for the Raman spectrums in Figs. S1 and S2. [5]. Moreover, the stains built around the bubble for the observed red-shifted G and 2D peaks by 7 cm-1 and 18 cm-1 are estimated to be around 0.2% and such strain is too small to cause any significant changes on the electronic properties of graphene, such as the formation of the second resistance peak in multi-probe transport measurements [5]

B. Temperature dependent charge transport behaviors of graphene bubble

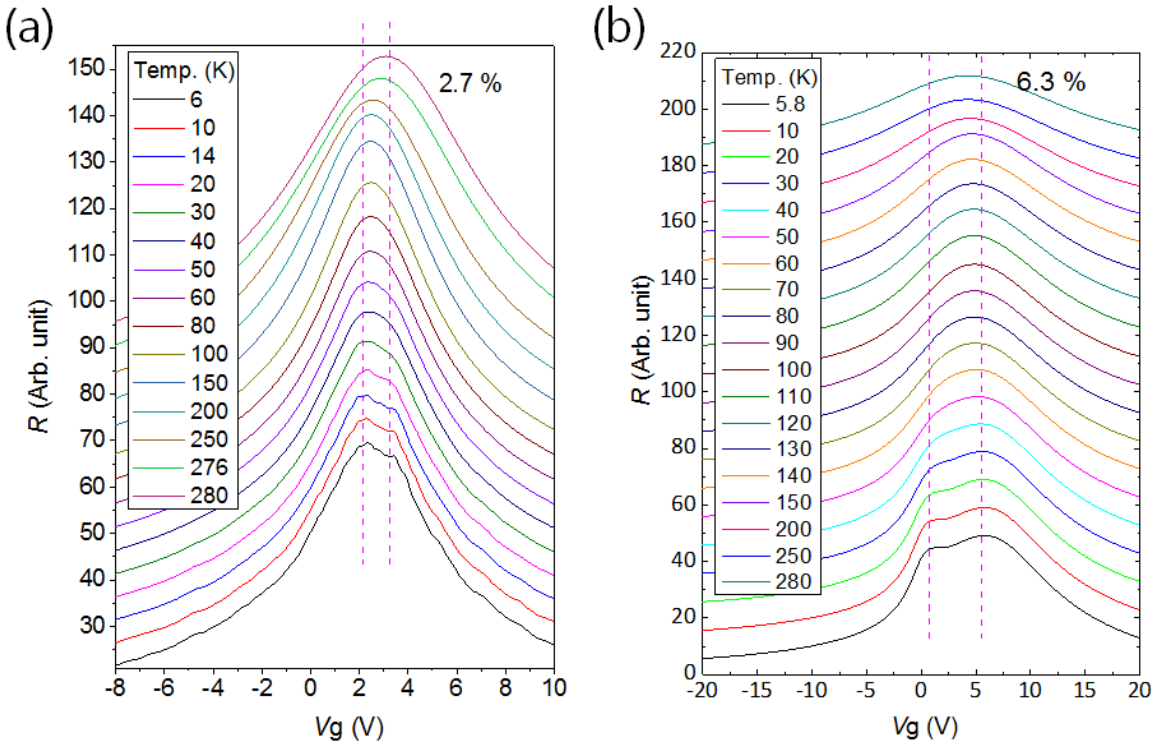

Figures S3 (a) and (b) show the series of charge transport characteristic curves from the multi-probed graphene devices with 2.7% and 6.3% of bubble coverages with varying temperatures. As presented in the main text, the first and the second resistance peaks are clearly resolved at low temperatures. As temperature increases, however, both peaks are merged into a single resistance peak whose width becomes wider accordingly. The transition temperature is determined by the interplay of the charge transports through bubble-free and bubble-rich graphene channels, but detailed analysis is out of the scope of the current report.

C. Numerical fitting for the graphene-*h*-BN device with an 8.7% bubble coverage

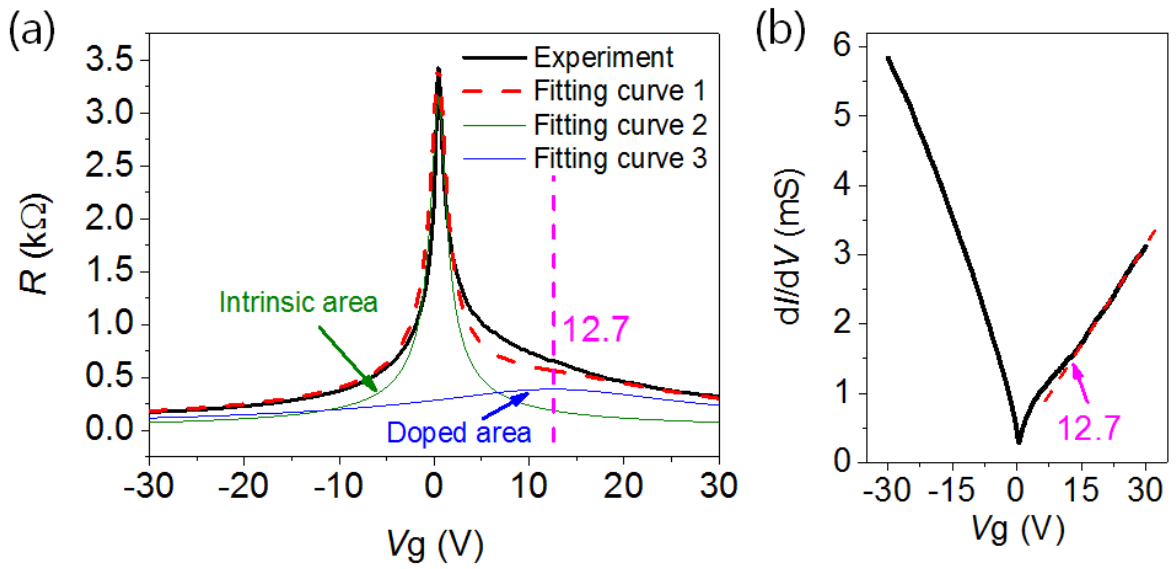

References

1. Yoon, et al., Strain-Dependent Splitting of the Double-Resonance Raman Scattering Band in Graphene, Phys. Rev. Lett. **106**, 155502 (2011)

2. Q. Hao, et al., Tuning surface-enhanced Raman scattering from graphene substrates using the electric field effect and chemical doping, Appl. Phys. Lett. **102**, 011102 (2013).

3. Dominik Metten, et al, All-Optical Blister Test of Suspended Graphene Using Micro-Raman Spectroscopy, Phys. Rev. Appl. **2**, 054008 (2014)

4. F. Fromm, et al., Looking behind the scenes: Raman spectroscopy of top-gated epitaxial graphene through the substrate, New Journ. of Phys. **15**, 113006 (2013)

5. M. Huang, Electronic-Mechanical Coupling in Graphene from in situ Nano indentation Experiments and Multiscale Atomistic Simulation, Nano Lett., 11, 1241 (2011)